Journal of Thermal Analysis, Vol. 47 (1996) 1267-1288

CONSTRUCTION OF A WHEAT-FLOUR STATE DIAGRAM
Application to extrusion processing

G. Kaletunç and K. J. Breslauer

Department of Chemistry, Rutgers, the State University of New Jersey, Piscataway, NJ 08855-0939, USA

Abstract

We use pressure-variable differential scanning calorimetry to detect and characterize thermally induced transitions (glass, melting, gelatinization) in pre- and post-extruded wheat flour. The resulting data allow us to construct a two-dimensional state diagram which maps the physical states that pre- and post-extruded wheat flour can assume, at constant pressure, as a function of moisture content, temperature, and the specific mechanical energy, SME, generated in the extruder. We describe how this state diagram can be used to map the path of extrusion processing, to assess the impact of extrusion conditions, and, ultimately, to design formulations and processing conditions that result in desired end-product attributes. For the extrudates, we find that the extent of processing-induced fragmentation, as monitored by reductions in the extrudate glass transition temperature, T_g, increases with the SME generated in the extruder. We demonstrate that a wheat–flour state diagram, which includes the glass curve of the wheat-flour extrudates produced at various SME values, allows one to predict and control the impact of processing conditions on extrudate properties.

Keywords: extrusion, state diagram, wheat flour

Introduction

The development of a fundamental understanding of the influence of processing and storage on food products requires studies which elucidate how the physical properties of food materials vary as a function of conditions which simulate processing and storage environments. These conditions can range from the relatively mild environments associated with food storage to the extreme conditions frequently encountered during extrusion processing (e.g. applied thermal and mechanical stresses at low moisture contents). The data which result from such studies can be used to construct multidimensional state diagrams, which describe the states of a material prior to and during processing. Similar state diagrams for the corresponding products can be constructed and used to assess the physicochemical changes which result from processing as well as product storage.

An understanding of the effects of processing and storage on the physical properties of food materials should allow one to predict and ultimately adjust,

0368–4466/96/ $ 5.00

John Wiley & Sons, Limited
Chichester

in a rational fashion, the formulation of raw materials and the processing parameters, so as to achieve desired end-product attributes. A knowledge of correlations between the physical properties of food materials and end-product sensory attributes also should provide a rapid and objective means for assessing the quality of food materials, with the overall goal of maintaining or improving quality. To achieve these goals, one first must develop a database *via* systematic studies in which the physical properties of food materials are characterized as a function of variables which are relevant to processing and storage conditions. The resulting database then can be used to construct multidimensional state diagrams which map the impact of processing and storage on end-product attributes [1].

As early as 1966, White and Cakebread [2] recognized the importance of characterizing the physical state(s) of sugars in sugar-containing food products to interpret some of the defects associated with changes in storage conditions (e.g., temperature, relative humidity). These investigators discussed the implications of the breakdown of the glassy state on the quality, safety, and storage stability of boiled sweets, milk powder, ice cream, and some freeze-dried products. Since 1966, numerous other researchers have measured fundamental properties (thermodynamic, rheological, kinetic) to define the physical states of food components under conditions which simulate processing and storage. Because the nature of these physical states can be related to the quality, shelf life, and sensory attributes of the end products, physical characterization of food components has received growing attention in the food science literature. This literature recently has been reviewed by Slade and Levine [3].

Over the years, a number of investigators have proposed that state diagrams (which map the physical states a material can assume as a function of concentration, temperature, pressure, and time) can be used to develop a fundamental understanding of food products and processing [4–8]. Specifically, Franks and coworkers [4] developed state diagrams for hydrophilic polymers, in connection with their use as cryoprotectants in the preservation of biological structure. Levine and Slade [5] described the application of an idealized state diagram for a hypothetical small carbohydrate to explain and/or predict the functional behaviour of such carbohydrates in frozen foods, in connection with cryo- stabilization technology. These researchers proposed that the glass transition should be considered the critical reference point, because various food materials are in an amorphous state. Roos and Karel [6] discussed the use of a "generic", simplified state diagram for a water-soluble food component to show the effect of temperature and moisture content on stability and material characteristics. They also suggested the possibility of using such diagrams to map the path of various food processes, as had Slade and Levine [7].

Recently, Slade and Levine [8] demonstrated that a sucrose-water state diagram (which reveals the relative locations of the glass, solidus, liquidus, and vaporus curves) is useful for characterizing various aspects of cookie and

cracker manufacturing, including dough mixing, lay time, machining, and baking, as well as for characterizing finished-product texture, shelf life, and storage stability. In a very recent review, Roos [9] reemphasized the use of glass transition temperature (T_g) values to establish state diagrams which describe the effect of composition on stability and which show the effects of temperature and moisture on viscosity, structure, and crystallization.

The above literature survey reveals that considerable attention has been directed towards characterizing the physical properties of food materials as a function of conditions relevant to food processing and storage. Extrusion, a frequently employed form of processing, is a high temperature, high shear cooking process that finds wide application in the food industry for preparation of breakfast cereals and snack foods. Starch- and protein-based cereal flours are frequently encountered as major components of the raw material mixtures for extrusion processing. As extensively discussed in a recent review by Slade and Levine [10], there have been a number of studies designed to characterize the thermally induced transitions (glass, melting, gelatinization, crystallization) in individual biopolymer components of cereal flours, as well as the influence of water on these transitions, with the ultimate goal of developing an understanding of structure-function relationships. Use of thermal data on individual components to interpret complex systems, such as studied here, ignores interactions between the components and the potential alteration of component thermal properties which might occur as a result of the separation process. Because wheat flour is a complex mixture of interacting biopolymers, the flour itself provides the appropriate thermodynamic reference state for extrusion-induced alterations in the thermal properties of the extruded material. We have designed and executed experiments to elucidate the differential thermal properties of pre- and post-extruded wheat flour (a real food system) as a function of plasticizing water. One of the primary objectives of the study reported here is to develop a state diagram for wheat flour, with the goal of characterizing the physical state of the wheat flour prior to, during, and after extrusion processing. To focus on the effects of two specific variables of interest, namely temperature and moisture content, we have used our experimental data to construct a simplified, two-dimensional state diagram for wheat flour. Differential scanning calorimetry (DSC) was used to detect and define those temperatures which correspond to significant thermally induced transformations (glass, melting, and gelatinization transitions), over temperature and moisture content ranges which simulate extrusion processing. Curves on the state diagram, which define the moisture-content dependence of these transition temperatures, form the boundaries between regions which correspond to particular states of the wheat flour. To exemplify how these data can be exploited to broaden our understanding of cereal flour processing, we have mapped on this state diagram the path of a high temperature extrusion cooking process. We also have placed the T_g values of wheat flour extrudates on the state diagram to assess the impact of shear, in terms of specific mechanical energy (SME), on the wheat flour during extrusion processing.

The results reported here build on and expand our understanding of the influence of SME on wheat flour fragmentation, which can be monitored by reductions in T_g. Consistent with our previous study on corn flour extrudates [1], we found in this work that the T_g values of wheat flour extrudates decrease with increasing SME generated in the extruder. In conjunction with the relationship between T_g and the sensory attribute, crispness, [1], which we have observed for corn flour extrudates, our wheat–flour state diagram can be used to define processing conditions which yield extrudates with desired sensory attributes. Furthermore, because our wheat–flour state diagram covers wide ranges of temperature (0–230°C) and moisture content (0–70%), it can be used to characterize other processes, such as pasta extrusion, for which wheat flour is a raw material.

Experimental

Materials

Hard wheat flour was obtained from Bay State Milling Co. (Winona, MN). According to the analysis provided by the supplier, the wheat flour contained 11.4% protein and less than 1% lipid. Amylose-to-amylopectin ratio of starch present in the wheat flour was 1:3. We determined the moisture content of the wheat flour to be 8 to 9% by freeze-drying. All percentages reported in the text are by weight, on a wet basis, with reference to the moisture content measured by freeze-drying.

Extrusion

Wheat flour was extruded in a corotating, self-wiping, twin-screw extruder with a barrel diameter of 30.9 mm (Werner & Pfleiderer, model ZSK-30, Ramsey, N.J.). The extruder barrel consists of five zones. Each zone is heated by resistive electric heaters and is equipped with an independent temperature control. The outside diameter (D) and total length (L_{total}) of each screw are 30.7 mm and 878 mm, respectively, with a L_{total}/D equal to 29.3. Each screw had forward conveying elements ($L_{convey}/D=21.9$), two mild mixing elements at 210 and 336 mm ($L_{mild\ mixing}/D=2.7$), six kneading elements at 434, 504, 618, 688, 766, and 780 mm ($L_{kneading}/D=3.6$), and two reverse elements ($L_{reverse}/D = 1.1$). The die diameter and length were 3 mm and 15 mm, respectively.

Wheat flour was fed into the extruder using a loss-in-weight feeding system (K-Tron Corp., Pitman, N.J.). Water was introduced to the extruder immediately after the flour feed zone. The extrusion process moisture levels specified in Table 1 were adjusted with a metering pump (US. Electric Motors, Milford, CT). A TPT 463E-10M transducer (Dynisco, Sharon, MA) was used to measure the temperature and pressure of the extrudate at the die.

Mass flow rate and screw speed were adjusted to yield different SME values, which were calculated using the following equation:

$$SME = \frac{\text{Torque} \times \text{screw speed}}{\text{mass flow rate}}$$

A total of six test runs was performed, encompassing two die temperatures and two feed-moisture levels. Table 1 outlines the extrusion process moisture, screw speed, total mass flow rate, extrudate temperature at die, and SME values for the six test runs on wheat flour.

Table 1 Extrusion operating conditions

Sample No.	Screw speed/ rpm	Total mass flow rate/ g min^{-1}	Extrudate temp. at die/ °C	SME/ kJ kg^{-1}
		Extrusion process moisture: 16%		
E1	500	225	160	1016
E2	300	400	160	554
E3	300	225	185	432
		Extrusion process moisture: 20%		
E4	500	225	185	416
E5	300	225	160	331
E6	300	400	185	236

Sample preparation for DSC experiments

A state diagram for wheat flour was constructed over a moisture content range of 0 to 70%. Freeze-drying was used to determine the initial moisture contents of the pre- and post-extruded wheat flour and to prepare dry flour and extrudate samples for DSC experiments. All extruded samples were ground with a mortar and pestle prior to DSC measurements.

Wheat flour samples of up to 18.7% moisture content were prepared by equilibration in dessicators over various saturated salt solutions for 48 h. The salts used were LiCl, $KC_2H_3O_2$, $MgCl_2$, NaCl and KNO_3. Saturated solutions of these salts at 25 °C produce relative humidity environments of 11, 23, 32,75, and 93%, respectively [11]. The sample moisture contents after equilibration were determined by measuring increases in sample weight. Corresponding equilibrated moisture contents of the wheat flour samples were 6, 7.8, 8.9, 14.7, and 18.7%. The samples of higher moisture content (up to 70%) were prepared by mixing wheat flour and water.

DSC experiments

DSC curves of wheat flour and its extrudates were recorded using a computer-controlled, pressure-variable, differential scanning calorimeter (DSC 111,

Setaram, France). This instrument allowed us to heat the samples over selected temperature ranges, while maintaining a predetermined, controlled pressure. The ability to maintain a constant pressure is a feature which distinguishes this calorimeter from conventional DSC instruments and permits a true measurement of specific heat capacity (C_p) as a function of temperature. The pressure was held constant at 30 atm during the DSC measurements, thereby shifting the water-vaporization peak outside the temperature range within which the thermal transitions of the pre- and post-extruded wheat flour are observed. All DSC measurements were conducted using fluid-tight, stainless steel crucibles with controlled-pressure environments. An empty crucible identical to the sample crucible was used as a reference. The sample and reference crucibles were heated at 5°C min^{-1} from 1 to 150°C, cooled to 1°C at 20°C min^{-1} equilibrated at 1°C for 2 h, and then heated a second time to 220°C. This procedure eliminates differences due to the thermal history of the sample, as well as obliterates an overlapping irreversible endothermic transition present at approximately 40–60°C in the 1st heating scan. Pressure-variable DSC provides the advantage of maintaining the moisture content of the samples constant during the heating and cooling scans. Melting and gelatinization temperatures were determined from a single-scan experiment to 220°C, because these transitions are irreversible.

DSC curves were normalized to yield the specific heat capacity as a function of temperature. The transition temperatures for the thermally induced transformations (e.g. glass, melting, and gelatinization transitions) in wheat flour samples and the glass transition in wheat flour extrudates were determined from the heat capacity curves. All T_g values were determined from the inflection point of the specific heat capacity *vs.* temperature curve taken from the second heating scan. The inflection point which corresponds to T_g was taken to be the temperature corresponding to the peak in the dC_p/dT *vs.* T curve. The peak temperatures of the endotherms for ice melting, starch melting, and starch gelatinization are reported as the corresponding transition temperatures.

Results and discussion

To characterize the impact of processing on a raw material, one can construct multidimensional state diagrams for the raw material and the product. As discussed by various authors [5, 6], the establishment of a state diagram for a raw material requires one to characterize thermally induced transitions as a function of temperature, pressure, moisture content, time, and additives. To assess the impact of processing, one must construct a complementary multidimensional state diagram for the product. The dimensions of this product state diagram, in addition to those listed above, also must include the processing parameters. The high dimensionality of such complete state diagrams makes interpretation and application of these data difficult. Consequently, as described

below for wheat flour, it is desirable to develop simplified state diagrams of lower dimensionality.

In this study, the thermal properties of wheat flour, as measured by pressure-variable DSC, were used to construct a state diagram. To eliminate the effect of changes in pressure during the heating scan, thereby simplifying the state diagram, we kept the pressure constant over the entire temperature range of DSC measurements. Pressure-variable DSC allowed us to heat samples adiabatically at a predetermined, controlled pressure over a selected temperature range. The capability to conduct experiments at a defined and controlled pressure is important and contrasts with conventional DSC instruments. In a conventional DSC, the sample is sealed in a cell and thus experiences an uncontrolled increase in pressure with increasing temperature (a pressure-cooker effect). In addition, in a conventional DSC, for samples with high moisture contents, the upper temperature limit of the experiment is dictated by the sample pan's ability to withstand the pressure developed (around 11 atm). However, in a pressure-variable DSC, the upper temperature limit is dictated by thermal decomposition of the sample. This becomes a highly practical feature, especially when we conduct our measurements under high temperature/pressure conditions which simulate extrusion processing. The simplified wheat–flour state diagram described below maps the influences of moisture content and temperature on the physical state of wheat flour at constant pressure. We also describe below how this diagram can be used to map the path of extrusion processing, to assess the impact of extrusion processing conditions, and, ultimately, to design processing conditions to achieve desired end-product attributes.

Wheat–flour state diagram

Figure 1 shows a simplified two-dimensional (temperature and moisture content) wheat–flour state diagram at 30 atm pressure. This diagram maps the various physical states that wheat flour can assume as a function of its moisture content and the temperature to which it is subjected. Changes between these states appear as apparent anomalies in the temperature dependence of the specific heat capacity of the material. Being a partially crystalline polymer system, wheat flour displays thermally induced transitions typical of both amorphous and crystalline materials. We have placed on Fig. 1 the transition temperatures of the calorimetrically detected, thermally induced transitions as a function of moisture content, to construct melting, gelatinization, and glass curves for wheat flour and a melting curve for the freezable water. Although wheat flour is a mixture of biopolymers, we could observe a single, apparent T_g in our DSC studies. This does not necessarily mean that there is only one glass transition. However, if the energy associated with any glass transition, which manifests itself as a heat capacity change, is small enough, that particular transition may not be detectable.

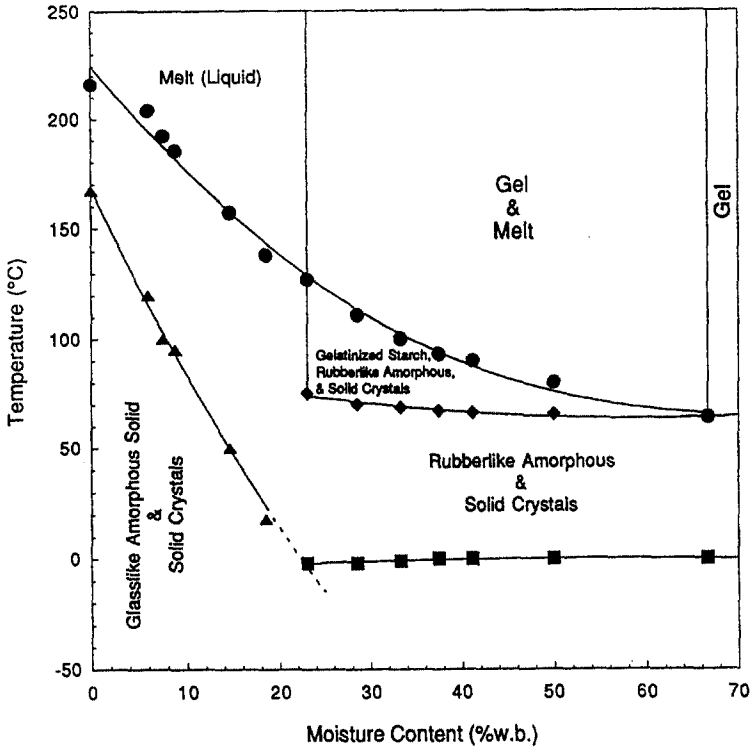

Fig. 1 Two-dimensional wheat–flour state diagram at 30 atm, showing the temperatures which correspond to the calorimetrically detected, thermally induced transitions (glass, melting, and gelatinization) as a function of moisture content; • T_m, ▲ T_g, ♦ T_{gel} for wheat flour, and ■ T_m for ice

Inspection of Fig. 1 reveals the influence of water as a plasticizer, a property which is apparent from the decreases in both T_g and melting temperature, T_m, with increasing moisture content. Specifically, as the moisture content of the wheat flour increases from 0% to 20% (a range over which T_g can be measured with our calorimeter), the value of T_g drops rapidly by about 8°C/(% of moisture added). A similar extent of water plasticization [~7.3°C/(% of moisture added), up to 20%] is evident from the T_g *vs.* starch concentration curve for rice starch, a partially crystalline biopolymer system, reported by Biliaderis [12]. Slade and Levine [13] have discussed the influence of water as a plasticizer on water-compatible, amorphous and partially crystalline polymers, an effect which has been observed by a number of investigators as a depression in T_g. Typically, at low moisture content (~< 10% water), a 5–10°C/(% of moisture) reduction of T_g is reported. Recently, Kalichevsky *et al.* [14, 15] published glass transition curves for amorphous amylopectin samples with moisture contents in the 10–25% range and for amorphous wheat gluten samples with moisture contents up to 16%. Both studies demonstrated that the T_g-depressing effect

of water continues beyond the 10% moisture content range [7°C/(% of moisture), over 10–25% moisture, for amylopectin [14] and 10°C/(% of moisture), over 0–16% moisture, for wheat gluten [15]], in agreement with our studies on wheat flour.

Further inspection of Fig. 1 also reveals that plasticization can be achieved by increasing the temperature at a constant moisture content, as well as by increasing the moisture content at a constant temperature. At constant moisture content, as the temperature increases, the amorphous regions of wheat flour go through a glass transition, leading to an increase in the translational and rotational motions of the polymer chains, due to an increase in volume. Similarly, the addition of moisture at constant temperature results in an increase in the segmental mobility of polymer chains, due to an increase in free volume and/or replacement of polymer–polymer hydrogen bonds by more labile water–polymer hydrogen bonds [13]. Such enhanced mobility in the system leads to relaxation of structure at a lower temperature, and thus a lower T_g.

At a moisture content lower than 20%, a high temperature endotherm appears in the DSC curves, which corresponds to the melting of crystalline regions of wheat flour. The transition temperature of this melting endotherm (T_m) shifts to lower temperatures as the moisture content of the wheat flour increases. At temperatures above the melting curve defined by T_m values as a function of moisture content, a free flowing, amorphous liquid state is reached. A second endotherm begins to appear, above 23% moisture, at temperatures below the high temperature melting endotherm. The transition temperature of this second endotherm (T_{gel}), which frequently is referred to as the gelatinization endotherm, is not as sensitive to moisture content as is T_m. At about 67% moisture, the two endotherms coalesce into a single endotherm, the transition temperature of which is independent of further increases in moisture content. Several models have been proposed to explain the phenomenon of multiple endotherms in thermal studies of starches. These issues have been reviewed by Biliaderis [12].

A complete characterization of wheat flour requires further investigation. In addition to the two important variables (temperature and moisture content) studied in this work, a complete simulation of processing and storage conditions should include characterization of the effects of time, composition of wheat flour, and additives. Levine and Slade [5] suggested that a time axis be included in the state diagram to describe kinetically controlled phenomena in the rubbery state that is often reached during processing and under some storage conditions. Wheat flour is expected to show compositional changes, depending on the region, season, and cultivar. We believe that further research, focusing on a systematic study of physical properties of wheat flour as a function of protein, lipid, and starch contents and amylose–amylopectin ratio, is needed to assess the extent of composition-induced changes in the physical properties. In a re-

cent study of corn flour extrudates, we have shown that addition of sucrose will decrease the T_g of extrudates, resulting in a loss of crispness [16]. Such information can be used to adjust the formulation and/or processing conditions in a rational fashion.

In summary, a fundamental understanding of the physical properties of preprocessed material, as embodied in a state diagram, is important, so that in conjunction with subsequent studies on extrudates, as described below, one can predict the impact of processing on the physicochemical properties of food materials. Armed with this ability, one should be able to control the processing conditions to improve the quality and stability of products.

The impact of extrusion processing on wheat flour

Mapping the path of extrusion processing

High temperature cooking-extrusion processing is used to manufacture ready-to-eat (RTE) cereals and snacks. Cereal and snack manufacturers often prefer extrusion processing over other processing techniques, because it creates highly expanded products, produces a wide variety of shapes and textures, cooks in a single processing step, and allows processing at relatively low moisture contents. For these reasons, it is desirable to elaborate the state diagram shown in Fig. 1 to include extrusion processing, as described below.

Figure 2 shows the wheat–flour state diagram on which we have superimposed the path of the high temperature cooking-extrusion process. This state diagram contains information relevant to the steps of extrusion processing (mixing of flour and water, high temperature cooking, puffing, and cooling), as well as to the final extrudate texture and storage stability. Prior to extrusion, wheat flour is primarily in a glassy state, but includes some crystalline regions. Water added prior to extrusion leads to extrusion moistures which typically range from about 15% for production of puffed snacks to 20–25% for production of RTE cereals [17]. Upon mixing with water, amorphous regions of the flour become plasticized. In fact, at high moisture, the wheat flour goes through its glass transition and becomes rubbery even at room temperature.

Cooking-extrusion normally requires temperatures higher than 150°C. Because of the high shear generated at fairly low moisture contents, the conversion of mechanical energy applied to wheat flour can go beyond thermal dissipation towards molecular energy storage [18]. Thermal dissipation results in an increase of temperature in the extruder. Stored molecular energy can result in polymer deformation, followed by elongation, and ultimately, bond rupture leading to fragmentation [18]. Depending on the level of applied mechanical energy, the extent of fragmentation in wheat flour varies. Discussion of processing-induced fragmentation will be deferred to a later section. With the increased temperature in the extruder, the crystalline regions of wheat flour melt, and ul-

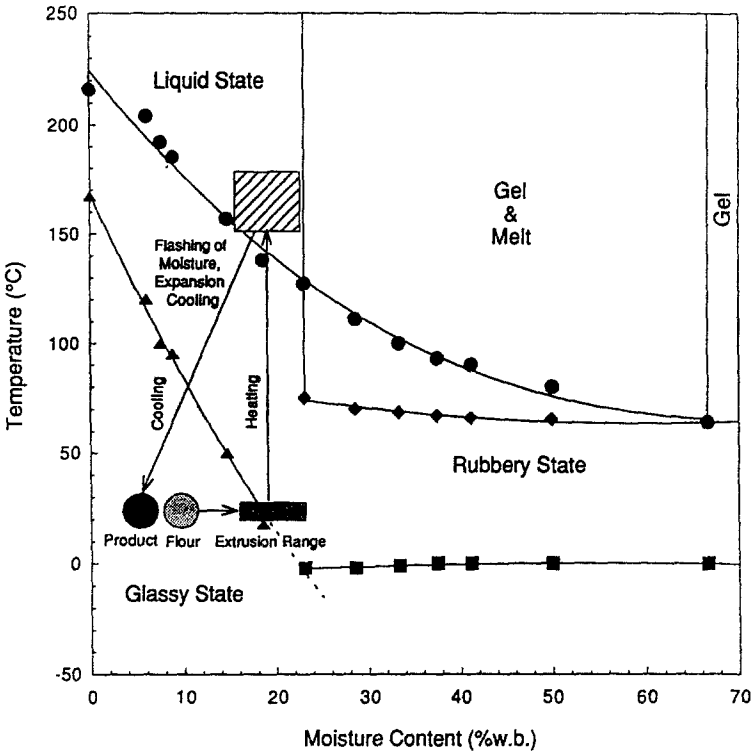

Fig. 2 The wheat–flour state diagram on which the path of a high temperature extrusion process is superimposed. The symbols are the same as in Fig. 1

timately, a free-flowing liquid state is reached. It should be recognized that calorimetric T_m values marked on the state diagram may only provide approximations for extrusion-based melting temperatures. As the extrudate exits the die, it expands due to die swell [19], vapor pressure-driven bubble growth, and flashing-off of moisture. The extrudate cools as a result of heat loss to the surroundings and vaporization of moisture, and reaches a rubbery state. Expansion continues in the rubbery state until a critical temperature; at this temperature, the pressure within the bubble is reduced to below atmospheric pressure [20]. Mitchell *et al.* [20] claim that the extrudate experiences a shrinkage with cooling below the critical temperature, because a partial vacuum is created within the bubble. Fan *et al.* [21] proposed a computer model to simulate bubble expansion followed by shrinkage, assuming that vapor pressure is the dominant factor. Their calculations showed that bubble-wall movement ceased when extrudate temperature fell below T_g+30 K. As the extrudate cools further toward ambient temperature, it goes through its glass transition and assumes a glassy state. In the glassy state, depending on the difference between ambient temperature and T_g, molecular motions are largely restricted to vibrations and short-range rotational motions. Consequently, extrudates can maintain the expanded

shape which they assume after extrusion. Because the transitions between these states are kinetically controlled, and various states are achieved before temperature equilibrium is reached, it should be emphasized that for complete characterization, time must be incorporated as another dimension in the state diagram.

The temperature and moisture content ranges covered by the wheat–flour state diagram presented here correspond to those applied to cereal flours as part of many food-processing operations, such as baking, pasta extrusion, and high temperature cooking-extrusion. In addition to its application to high temperature extrusion processing, as described above, our wheat–flour state diagram also can be and has been used to map the path of pasta-extrusion processes (unpublished results). In fact, along any of the processing paths listed above, one can determine the physical state of the wheat flour by locating the intersection of the temperature and moisture content values corresponding to a given stage of the process. For any raw material, such a diagram can be used as a predictive tool for evaluating the performance of that material during processing. This predictive ability, prior to processing, enables one to improve performance, if necessary, by changing processing conditions and/or changing the formulation, so as to favor desired end-product attributes.

Placement of extrudates on the wheat–flour state diagram

We have shown previously that the T_g values of extrudates can be related to product sensory attributes [1]. Here, we develop further correlations between the thermal properties of raw materials and products, so as to develop a predictive capability which will permit rational adjustments of raw material formulations and processing conditions to yield desired end-product attributes.

During processing, irreversible changes may occur and new structures may develop. Thus, a complete characterization of the impact of processing requires construction of state diagrams for both the raw materials and products. To this end, we have used DSC to evaluate the thermal properties of wheat flour extrudates. By comparing the wheat flour data described earlier with DSC data on extrudates, we have evaluated the effects of extrusion processing on the wheat flour as a function of SME. Specific heat capacity *vs.* temperature curves of extrudates produced at various SME values and extrusion moistures were constructed (data not shown). These curves revealed the only thermal transition observed for the wheat flour extrudates to be a glass transition, which is characteristic of an amorphous material. This result was in agreement with an expectation based on our earlier X-ray diffraction studies on corn flour extrudates, which showed those extrudates to be amorphous, since they contained no X-ray peaks characteristic of crystalline material [1]. Using polarized-light microscopy, Politz *et al.* [22] reported the absence of birefringence for the same wheat-flour extrudates, indicating absence of ordered structure.

Figures 3 and 4 are expanded views of the wheat–flour state diagram. In these figures, we superimposed the path of the extrusion process (open symbols), in terms of the various extrusion operating conditions described in Table 1. We also placed the T_g values of the extrudates at their measured moisture contents (the corresponding filled symbols) on the diagram.

Comparison of Figs 3 and 4 shows that the two sets of samples, which differed by the amount of added water, began the extrusion process from different regions of the state diagram. Note that with addition of water up to 16%, wheat flour is plasticized but still in the glassy state (Fig. 3), while at 20% extrusion moisture, the wheat flour goes through its glass transition and becomes rubbery at ambient temperature (Fig. 4). At the two extrusion moisture levels examined, different SME ranges were achieved, as listed in Table 1. This difference in SME led to different extents of fragmentation of the wheat flour, as reflected in variations in T_g of the extrudates [1]. It is apparent from Figs 3 and 4 that, independent of the extrusion conditions, all of the extrudates were in the glassy state at room temperature and moisture contents of 7 to 9.5%. In addition, we

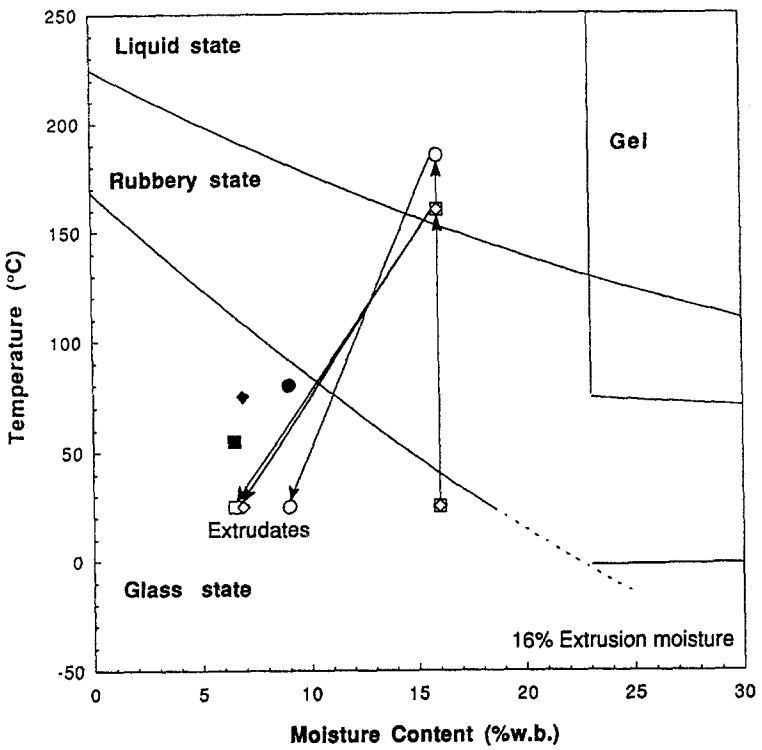

Fig. 3 Expanded view of the wheat–flour state diagram. Paths of the extrusion process (open symbols) at various SME values are superimposed. T_g values of the extrudates at their measured moisture contents (the corresponding filled symbols) are indicated. □■ 1016 kJ kg^{-1}, ◊♦ 554 kJ kg^{-1}, o• 432 kJ kg^{-1}

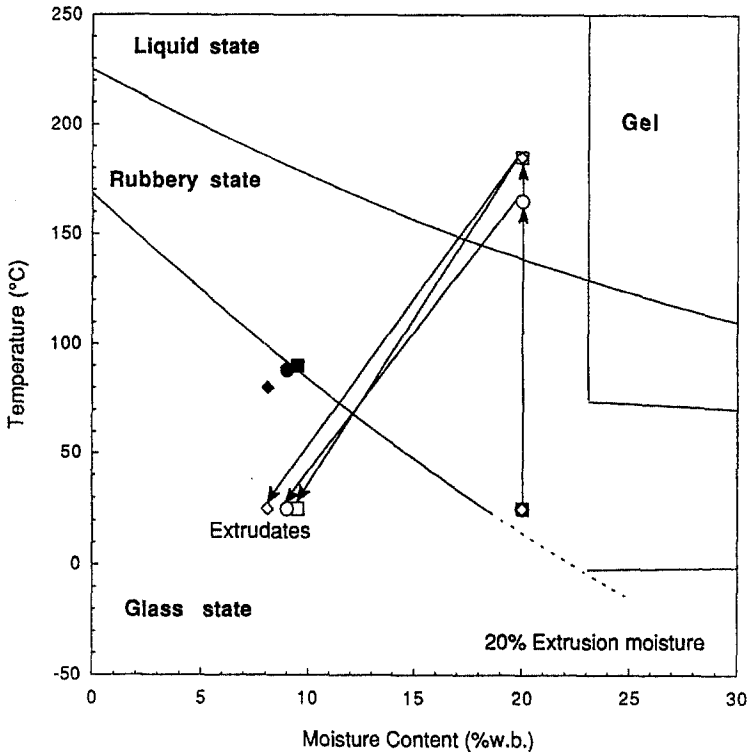

Fig. 4 Expanded view of the wheat–flour state diagram. Paths of the extrusion process (open symbols) at various SME values are superimposed. T_g values of the extrudates at their measured moisture contents (the corresponding filled symbols) are indicated. ◊ ♦ 416 kJ kg^{-1}, o • 331 kJ kg^{-1}, □ ■ 236 kJ kg^{-1}

observed that the T_g values of these extrudates were lower than those of wheat flour with comparable moisture contents. However, the extent of the difference between the T_g values of the extrudate and wheat flour, which corresponds to the extent of fragmentation during extrusion, clearly depended on the SME generated in the extruder.

Predicting the influence of post-extrusion storage conditions

For highly fragmented extrudates, which display low T_g values, elevated storage temperature may induce the rubbery state. Moreover, an increase in the relative humidity of the storage environment may increase the moisture content of such extrudates, thereby leading to even lower T_g values, and thus to the rubbery state at even lower storage temperatures. If, as a result of increases in temperature and/or relative humidity of the storage environment, the extrudate reaches the rubbery state, the stresses maintaining the porous, expanded struc-

ture could relax and the extrudate could shrink, with a concomitant loss of crispy texture. To study the moisture-induced shrinkage of wheat-flour extrudates, we equilibrated two extrudate samples of cylindrical shape (with corresponding SME values of 356 and 518 kJ kg^{-1}) over saturated salt solutions which produced 42 and 93% relative humidity environments at 25°C. While we did not observe any decrease in length or diameter of either sample at 42% RH, in the 93% RH environment, extrudates did not retain their original expanded structure. Shrinkage was characterized by reductions in both length and diameter, although the change in volume was dominated by the reduction in the diameter of the extrudates (unpublished results). Thus, we can use our thermal stability data, in conjunction with data on macrostructural changes, to evaluate and predict the effects of post-extrusion storage conditions (temperature and relative humidity) on the state of the extrudate. Based on this capability, optimal storage conditions can be devised. Alternatively, the formulation and processing conditions can be adjusted in a rational way to enhance the storage stability of the product.

It should be emphasized that, in addition to the extrudate T_g values at various moisture contents, the moisture sorption characteristics of extrudates need to be determined. The wheat–flour state diagram, in conjunction with glass curves and water sorption isotherms of wheat-flour extrudates at various SME values, should allow one to predict and control the impact of processing conditions on extrudate properties.

Comparison of molecular weight and T_g data to detect fragmentation

Figure 5 shows how the T_g and weight-average molecular weight ($\overline{M}_w$) values of wheat-flour extrudates (the latter determined by gel permeation chromatography (GPC) [22]) depend on SME. Because T_g of the extrudate is very sensitive to its moisture content, T_g measurements were performed on freeze-dried extrudates, to investigate the influence of $\overline{M}_w$ at constant moisture content for all extrudates. The SME can be considered a measure of the extent of stress applied to the wheat flour. There is a clear decrease in T_g with increases in the applied mechanical stress, as quantified by SME. It is apparent that the $\overline{M}_w$ of extrudates also decreases as SME increases. We previously demonstrated that the extent of fragmentation in corn flour extrudates can be monitored by reductions in T_g of the extrudates [1]. The observation that processing-induced fragmentation is reflected in both the apparent molecular weight distribution and the temperature of the glass transition further emphasizes the utility of T_g as a means of assessing the extent of fragmentation in extruded cereal flours.

Closer examination of Fig. 5 reveals an apparent discrepancy between $\overline{M}_w$ and T_g of extrudates as SME increases from 554 to 1016 kJ kg^{-1}. Note that the molecular weight of the extrudates, as assessed by GPC, changes only slightly,

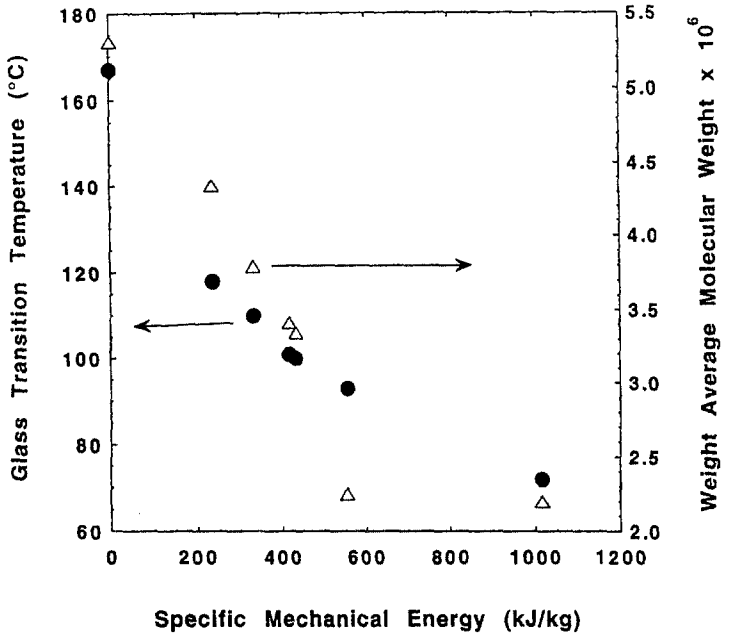

Fig. 5 SME dependence of T_g of freeze-dried wheat flour extrudates (•) determined by DSC and weight-average molecular weight of the wheat flour extrudates (Δ), determined by Politz *et al.* [22] using GPC

when the SME is increased from 554 to 1016 kJ kg^{-1} [22]. This trend suggests that an SME value of 1016 kJ kg^{-1} is close to the upper limit of the shearing force which induces fragmentation. It is expected that with increasing values of shear stress, the molecular weight of fragmented polymers should approach a lower limit [18]. In contrast to the negligible change in $\overline{M}_w$ observed over this range of SME, we observed a 20°C decrease in T_g. This result may imply that the limiting shear force had not been reached.

The dependence of T_g on the mechanical stress applied during the extrusion process, at SME values where the apparent molecular weight is no longer decreasing, may reflect differences in the sensitivity of the thermal and hydrodynamic observables to the processing-induced fragmentation of the extruded material. It has previously been emphasized by Colonna [23] that, although GPC gives quantitative results for the average molecular weight of polymers, the molecular weight distributions of very large or very small molecules are not determined accurately by this technique. The presence of very small molecules, as expected at a high SME value of 1016 kJ kg^{-1}, may not be detected by GPC. Thus, the thermal observable, T_g, may be sensitive to fragmentation which is not detected by conventional GPC methods. In fact, small fragments may act as plasticizers, thus making T_g a very sensitive indicator of their presence. An additional advantage of DSC-determined T_g values over GPC is that DSC can be

performed on solid samples, while GPC requires that the material be dissolved in a solvent. Clearly, further investigation is necessary to assess the dependence of the extent of fragmentation on the mechanical energy applied at higher levels of shear force, and to assess its relation to the physical properties and sensory attributes of the extrudates.

Molecular weight distribution affects the breadth of the glass transition

Specific heat capacity curves for all wheat-flour extrudates revealed that the transition from the glassy to rubbery state occurs over a broad temperature range. In addition to the multicomponent, heterogeneous nature of pre-extruded wheat flour, the breadth of the transition may originate from the heterogeneity created during extrusion, due to polymer fragmentation. Slade and Levine [7] noted that multi-component, complex food products, in which moisture and water-compatible solids are heterogeneously distributed, can have multiple amorphous domains with different T_g values. For starch, Biliaderis [12] emphasized the possibility of the presence of a range of nonordered domains, each manifesting its own T_g, and extending the glass transition of the multi-component material over a broad range of temperatures. In a recent review, Angell [24] discussed the possibility of multiple glassy states with different packings in glass-forming proteins and other biopolymers. In synthetic polymers, the existence of microphases with various polymer chain lengths was reported by Gaur and Wunderlich [25]. Wunderlich [26] attributed the observation of asymmetric broadening of the glass transitions of copolymers and block copolymers to the existence of these microphases and their attachment to each other. It is reasonably well established that T_g is related to the molecular weight of a polymer, and that the glass transition region can be interpreted qualitatively as the onset of long-range, coordinated molecular motion [27]. Different molecular weight fragments present in an extrudate will go through their glass transition at different temperatures. In the case of a broad molecular weight distribution, the glass transition for fragments of increasing molecular weight will occur at successively higher temperatures. It is possible that lower-weight fragments in the rubbery state may act as plasticizers for higher molecular weight fragments, thus decreasing T_g of the larger fragments. Consequently, the glass transition for wheat-flour extrudates may occur as a continuum over a broad temperature range. One should therefore recognize, when constructing and using state diagrams, that the glass transition occurs over a range of temperatures, and that regions of the diagram near T_g-defined boundaries may actually represent states which are mixtures of glassy and rubbery material.

SME, the major determinant of fragmentation

We [1] and others [28–31] have reported that processing-induced fragmentation of synthetic and biopolymers is related to mechanical forces. We have demonstrated for corn-flour extrudates that the extent of extrusion-induced

fragmentation is related to the SME generated in the extruder, and that such fragmentation can be monitored by observed reductions in T_g of extrudates. Superimposing the T_g values of wheat-flour extrudates on the wheat–flour state diagram, as shown in Figs 3 and 4, demonstrates the impact of shear during extrusion processing. As noted above, different SME values are achieved, depending on initial moisture content, mass flow rate, and screw speed. Even for the lowest SME value of 236 kJ kg^{-1}, fragmentation occurred in the extruder, with T_g values of wheat–flour and extrudate being around 98°C and 90°C, respectively, at about 9% moisture. It has been shown in a previous study on molten maize starch [32] that macromolecular degradation first appears when the mechanical energy reaches about 10^7 J m^{-3}. The lowest SME of 236 kJ kg^{-1} reported in the present work corresponds to ~10^8 J m^{-3}, which is above the minimum mechanical energy required to induce fragmentation. Thus, even at the lowest SME value studied here, some fragmentation was expected. At higher SME values, the difference between the T_g values of wheat flour and extrudate T_g becomes larger. Therefore, construction of state diagrams for products, as a function of a process parameter (SME) and moisture content, is necessary to predict the impact of physicochemical changes associated with processing conditions, as well as to predict the storage stability of extrudates.

As discussed earlier, SME is a process parameter which combines the effects of mass flow rate and screw speed, in addition to material properties, such as viscosity. The viscosity of a flour-water mixture in the extruder is affected by applied shear, temperature, and moisture content. Thus, SME is an important factor to evaluate the collective influences of various operating conditions (e.g. temperature, screw speed, mass flow rate, moisture content, and additives) on the extent of fragmentation. Politz and coworkers [22] reported that low extrudate temperatures at die result in extensive fragmentation. Our results, however, revealed that for extrudates with the same extrusion moisture, a sample with a temperature of 160°C at the die, but 236 kJ kg^{-1} SME, displayed a higher T_g and higher molecular weight (less fragmentation) than did a sample with a temperature of 185°C at the die, but 416 kJ kg^{-1} SME. This observation suggests that the collective effects of several operating conditions, conveniently parameterized by SME, are the major determinants of fragmentation. The influence of extrusion operating variables on extent of fragmentation is indirect. Each operating variable affects SME [16], and their combined effect, in terms of SME, defines the extent of fragmentation.

To evaluate further the impact of mechanical stress on extrudate physical properties, we examined the T_g of freeze-dried extrudates. Recall that Fig. 5 plots T_g as a function of SME for freeze-dried wheat-flour extrudates produced at 16 and 20% initial extrusion moisture contents. $\overline{M}_w$ values of wheat-flour extrudates, determined by Politz and coworkers [22] using GPC, are also plotted as a function of SME on Fig. 5. The T_g and molecular weight values of freeze-

dried, unextruded wheat flour correspond to a zero SME value. Note that T_g of the wheat-flour extrudates decreases as SME increases. Specifically, we observed a 46°C reduction in T_g over a 780 kJ kg^{-1} SME range (236–1016 kJ kg^{-1}), or a $\Delta T_g/\Delta$SME value of 0.059°C/(kJ kg^{-1}). In a previous study [1], we reported that T_g of corn-flour extrudates also decreased as SME increased; however, the quantitative impact, as assessed by $\Delta T_g/\Delta$SME, differed significantly for the two types of corn flour studied. We suggested that this difference may be related to the amylose-amylopectin ratios of the two corn flours.

Figure 6 shows the influence of SME on T_g, as a function of amylose-amylopectin ratio for wheat- and corn-flour extrudates. Note the increased sensitivity of T_g to SME with increasing amylose-amylopectin ratio. Because T_g is sensitive to molecular weight changes, this observation may indicate that stress-induced reduction in $\overline{M}_w$ values due to fragmentation is greater in high amylose flours than in high amylopectin flours. If in amylopectin, a branched biopolymer, fragmentation takes place primarily at branch points, the resultant small chain length fragments may not decrease $\overline{M}_w$ of the polymer as drastically as would the relatively large fragments produced by breakage of linear amylose chains. Porter and Casale [18] reported that the extent of stress-induced reaction depends on the imposed strain, chain topology, crosslink density, and chemical composition, and also that the junctions of long branches of branched polymers are most susceptible to stress reactions.

The impact of extrusion processing is more obvious for extrudates produced at 16% extrusion moisture, based on the deviation of their T_g values from the glass curve of the wheat flour–water system (Fig. 3). As noted previously and seen in Table 1, the SME achieved with a particular set of processing conditions depends on the initial moisture content of the wheat flour–water mixture. Interestingly, T_g values of extrudates with similar SME values (416 and 432 kJ kg^{-1}), but different extrusion moistures (20 and 16%, respectively), are indistinguishable. $\overline{M}_w$ for these two extrudates were reported to be virtually the same, $3.34 \cdot 10^6$ for 432 kJ kg^{-1} and $3.41 \cdot 10^6$ for 416 kJ kg^{-1} [22]. Thus, it is clear that, for a given flour, mechanical energy input is the main factor which determines the extent of fragmentation induced by extrusion.

Concluding remarks

We have demonstrated that a wheat–flour state diagram can be used to define the physical state of wheat flour prior to and during high-temperature extrusion processing. We determined the thermal properties of wheat flour over the temperature and moisture content ranges typically employed in extrusion processing, by using a pressure-variable DSC to detect and define temperatures corresponding to significant thermally induced transitions (glass, melting, and gelatinization) in wheat flour. From these data, we constructed a two-dimensional state diagram at constant pressure, which describes the physical states of wheat flour as a function of moisture content and temperature.

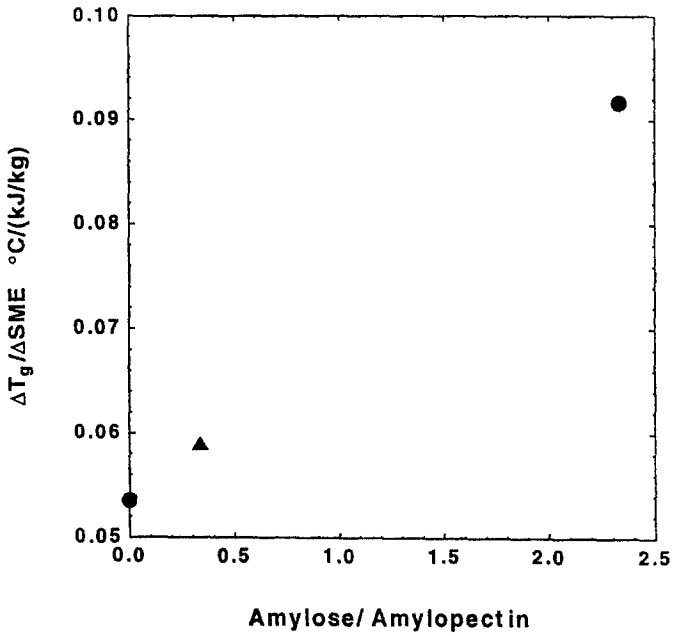

Fig. 6 Sensitivity of T_g to SME, as a function of amylose–amylopectin ratio for cereal flours; • corn flour, ▲ wheat flour

To assess the influence of shear on wheat flour during extrusion, we determined the thermal properties of wheat-flour extrudates as a function of various levels of mechanical energy, characterized by SME. A glass transition, characteristic of an amorphous material, was the only thermal transition observed for wheat-flour extrudates. We found the T_g values of wheat-flour extrudates to decrease with increasing SME generated in the extruder. We located these T_g values on the wheat–flour state diagram and compared the T_g values of unextruded wheat flour and wheat-flour extrudates at identical moisture contents, to assess the extent of fragmentation as a function of SME, as monitored by decreasing T_g. We note that, based on the wheat–flour state diagram and knowledge of the SME dependence of T_g, processing conditions can be adjusted to yield extrudates with desired T_g values. To make these correlations of practical value, one must have criteria for selection of the target T_g which relates to end-product attributes of significance to the consumer. In an earlier study on corn-flour extrudates, we demonstrated [1] that an increase in T_g is related to an increase in the sensory textural attribute of crispness, which is one of the major criteria by which a consumer judges the quality of a breakfast cereal or puffed snack product. Thus, knowledge of T_g values corresponding to desirable levels of product crispness can be of value to a manufacturer. In short, determination of the thermal properties of products, specifically T_g, can be useful for quality

control in the manufacture of such products. This approach has the advantages of being less costly, more rapid, and more objective than sensory measurements. In addition, knowledge of product thermal properties, together with the state diagram of raw materials, can be used to adjust processing conditions and/or formulation of raw materials to achieve desired end-product attributes and improve quality. For example, sucrose, a common additive in breakfast cereals, is known to act as a plasticizer [3]. We have shown by mechanical and thermal measurements [16] that sucrose plasticizes corn extrudates. Consequently, T_g of extrudates should decrease with the addition of sugar, resulting in a loss of crispness. Thus, a state diagram can be utilized to adjust extrusion processing conditions (e.g. by decreasing SME) to compensate for the T_g-depressing influence of sucrose. In addition to improving the quality of an existing product, one can use state diagrams as part of a rapid evaluation procedure in the product development area to judge the feasibility of potential products.

To define storage conditions (temperature, relative humidity) that enhance the stability and, therefore, the shelf life of extruded products, one can use moisture sorption isotherms in conjunction with glass curves of extrudates [1]. In fact, a state diagram for pre- and post-extruded cereal flour can be used in conjunction with the corresponding moisture sorption isotherms to define and adjust processing conditions, so as to produce extrudates with enhanced stability.

In summary, state diagrams have great potential in food product development, because they can provide a rational basis for designing processing conditions and/or raw material formulations, so as to favor desired end-product attributes.

* * *

This is publication D 10544-6-95 of the New Jersey Agricultural Experiment Station, supported by State funds and the Center for Advanced Food Technology of the New Jersey Commision on Science and Technology. The authors would like to thank Dr. G. Eric Plum for his comments on the manuscript and Dr. Karwe for producing extrusion samples.

References

1 G. Kaletunç and K. J. Breslauer, Cereal Chem., 70 (1993) 548.
2 G. W. White and S. H. Cakebread, J. Food Technol., 1 (1966) 73
3 L. Slade and H. Levine, in Advances in Food and Nutrition Research, Ed. J. E. Kinsella, Vol.38, Academic Press, San Diego 1995, p.103.
4 F. Franks, M. H. Asquith, C. C. Hammond, H. B. Skaer and P. Echlin, J. Microscopy, 110 (1977) 233.
5 H. Levine and L. Slade, Cryo-Letters, 9 (1988) 21 .
6 Y. Roos and M. Karel, Food Technol., 66 (1991) 68.
7 L. Slade and H. Levine, Crit. Rev. Food Sci. Nutr., 30 (1991) 115.
8 L. Slade and H. Levine, in The Glassy State in Foods, Ed. J. M. V. Blanshard and P. J. Lillford, Univ. Nottingham Press, Nottingham, UK 1993, p.35.
9 Y. Roos, J. Food Eng., 24 (1995) 339.

10 L. Slade and H. Levine, J. Food Eng., 24 (1995) 431.
11 L. Greenspan, J. Res. Nat'l Bureau Standards, (1976) 81 A.
12 C. G. Biliaderis, in Thermal Analysis of Foods, Ed. V. R. Harwalkar and C. Y. Ma, Elsevier Applied Sci., New York 1990, p.168.
13 L. Slade and H. Levine, in Food Structure–Its Creation and Evaluation, Ed. J. M. V. Blanshard and J. R. Mitchell, Butterworths, London 1988, p. 115.
14 M. T. Kalichevsky, E. M. Jaroszkiewicz, S. Ablett, J. M. V. Blanshard and P. J. Lillford, Carbohydr. Polym., 18 (1992) 77.
15 M. T. Kalichevsky, E. M. Jaroszkiewicz and J. M. V. Blanshard, Int. J. Biol. Macromol., 14 (1992) 257.
16 A. Barrett, G. Kaletunç, S. Rosenberg and K. Breslauer, Carbohydr. Polym., 26 (1995) 261.
17 J. M. Harper, in Extrusion Cooking, Ed. C. Mercier, P. Linko and J. M. Harper, Am. Assoc. Cereal Chem., St. Paul, MN 1989, p. 1.
18 R. S. Porter and A. Casale, Polym. Eng. Sci., 25 (1985) 129.
19 R. C. E. Guy and A. W. Horne, in Food Structure – Its Creation and Evaluation, Ed. J. M. V. Blanshard and J. R. Mitchell, Butterworths, London 1988, p.331.
20 J. R. Mitchell, J. Fan and J. M. V. Blanshard, Extrusion Communique, March (1994) 10.
21 J. Fan, J. R. Mitchell and J. M. V. Blanshard, J. Food Eng., 23 (1994) 337.
22 M. L. Politz, J. D. Timpa, A. R. White and B. P. Wasserman, Carbohydr. Polym., 20 (1994) 91.
23 P. Colonna, J. Tayeb and C. Mercier, in Extrusion Cooking, Ed. C. Mercier, P. Linko and J. M. Harper, Am. Assoc. Cereal Chem., St. Paul, MN 1989, p. 247.
24 C. A. Angell, Science, 267 (1995) 1924.
25 U. Gaur and B. Wunderlich, Macromolecules, 13 (1980) 1618.
26 B. Wunderlich, Thermal Analysis, Academic Press, New York 1990, p. 297.
27 L. H. Sperling, Introduction to Physical Polymer Science, 2nd ed., Wiley, New York 1992, p. 311.
28 R. T. Conley, in Thermal Stability of Polymers, Ed. R. T. Conley, Vol. 1, Marcel Dekker, New York 1970.
29 M. H. Gomez and J. M. Aquilera, J. Food Sci., 49 (1984) 40.
30 V. J. Davidson, D. Paton, L. L. Diosady and L. J. Rubin, J. Food Sci., 49 (1984) 1154.
31 K. Kim and M. K. Hamdy, J. Food Sci., 52 (1987) 1387.
32 B. Vergnes and J. P. Villemaire, Rheologica Acta, 26 (1987) 570.